Available online at www.sciencedirect.com
ScienceDirect
Geochimica et Cosmochimica Acta 71 (2007) 4629–4643
Geochimica et Cosmochimica Acta
www.elsevier.com/locate/gca

# Biogeochemistry of Fe(II) oxidation in a photosynthetic microbial mat: Implications for Precambrian Fe(II) oxidation

Robert E. Trouwborst [a], Anne Johnston [b], Gretchen Koch [c], George W. Luther III [a,*], Beverly K. Pierson [b]

[a] University of Delaware, College of Marine and Earth Studies, Cannon Laboratory 218, 700 Pilottown Road, Lewes, DE 19958, USA
[b] University of Puget Sound, Biology Department, 1500 North Warner, Tacoma, WA 98416, USA
[c] Pennsylvania State University, Department of Biochemistry and Molecular Biology, University Park, PA 16802, USA

Received 12 March 2007; accepted in revised form 6 July 2007; available online 16 August 2007

**Abstract**

We studied the role of microbial photosynthesis in the oxidation of Fe(II) to Fe(III) in a high Fe(II) and high Mn(II) hot spring devoid of sulfide and atmospheric oxygen in the source waters. *In situ* light and dark microelectrode measurements of Fe(II), Mn(II) and $O_2$ were made in the microbial mat consisting of cyanobacteria and anoxygenic photosynthetic *Chloroflexus* sp. We show that Fe(II) oxidation occurred when the mat was exposed to varying intensities of sunlight but not near infrared light. We did not observe any Mn(II) oxidation under any light or dark condition over the pH range 5–7. We observed the impact of oxygenic photosynthesis on Fe(II) oxidation, distinct from the influence of atmospheric $O_2$ and anoxygenic photosynthesis. *In situ* Fe(II) oxidation rates in the mats and cell suspensions exposed to light are consistent with abiotic oxidation by $O_2$. The oxidation of Fe(II) to form primary Fe(III) phases contributed to banded iron-formations (BIFs) during the Precambrian. Both oxygenic photosynthesis, which produces $O_2$ as an oxidizing waste product, and anoxygenic photosynthesis in which Fe(II) is used to fix $CO_2$ have been proposed as Fe(II) oxidation mechanisms. Although we do not know the specific mechanisms responsible for all Precambrian Fe(II) oxidation, we assessed the relative importance of both mechanisms in this modern hot spring environment. In this environment, cyanobacterial oxygen production accounted for all the observed Fe(II) oxidation. The rate data indicate that a modest population of cyanobacteria could have mediated sufficient Fe(II) oxidation for some BIFs.


## 1. INTRODUCTION

We studied the role of photosynthesis in the oxidation of Fe(II) in a hot spring associated with a growing iron deposit. High iron environments near neutral pH, which are exposed to light and not dominated by atmospheric oxygen are rare on Earth today. The mats we studied were at the source waters of an anoxic spring and, for a limited distance from the source, provided such an environment devoid of atmospheric oxygen. Our studies were designed to determine the activities of iron-tolerant phototrophs in a high iron natural setting. We measured parameters that could have implications for the biogeochemistry of iron(II) oxidation on an ancient Earth lacking an oxic atmosphere.

### 1.1. Study context

Banded iron-formations (BIFs) are massive deposits of iron minerals which formed between 3.8 and 0.8 Ga with a major deposition period from 2.8 to 1.8 Ga (Klein and Beukes, 1992). The average iron oxidation state of several of these formations is +2.4 (Klein and Beukes, 1992). The source of Fe(III) in early iron deposits is unknown. The mechanism of oxidation of Fe(II) to Fe(III) prior to an oxic atmosphere is the subject of much speculation. Several hypotheses have been proposed, including abiotic oxidation

* Corresponding author. Fax: +1 302 645 4007.
*E-mail address:* luther@udel.edu (G.W. Luther III).

0016-7037/$ - see front matter © 2007 Elsevier Ltd. All rights reserved.
doi:10.1016/j.gca.2007.07.018

by the higher UV fluxes in the Precambrian (Cairns-Smith, 1978; Braterman et al., 1983; François, 1986; Anbar and Holland, 1992) or by $O_2$ produced abiotically in the atmosphere (Berkner and Marshall, 1964; Brinkman, 1969; Towe, 1978). Three biological processes have been proposed. Direct chemotrophic oxidation of Fe(II) by iron-oxidizing bacteria which presumably used oxygen produced abiotically or by early cyanobacterial photosynthesis as an electron acceptor for respiration (Holm, 1987; Emerson and Revsbech, 1994a,b). Archean and Proterozoic phototrophs could have oxidized the Fe(II) and deposited Fe(III) minerals by two different photosynthetic mechanisms: (1) indirectly with oxygenic photosynthesis in which water is used as a reductant for $CO_2$ fixation and oxygen is produced as a waste product; or (2) directly with anoxygenic photosynthesis in which Fe(II) is used as a reductant for $CO_2$ fixation (photoferrotrophy). Note that the indirect photosynthetic mechanism biologically produces molecular oxygen which functions as the oxidant for Fe(II) oxidation. The actual oxidation process of the Fe(II) by the oxygen is abiotic. When we discuss the oxidation of Fe(II) by oxygen produced by cyanobacteria, we will describe the oxidation as abiotic.

Preston Cloud (1965, 1973) proposed that the appearance of the first ancestors of modern cyanobacteria capable of oxygenic photosynthesis were responsible for the early oxidation of iron in shallow ocean basins. Presumably all of the oxygen produced by these ancestral cyanobacteria was consumed by oxidizing soluble Fe(II) and other reduced substances. With an abundance of reduced iron, no oxygen accumulated, and the water remained anoxic with a low redox state. The oxidation of iron was thus a chemical process, the oxygen being provided by cyanobacterial photosynthesis (Cloud, 1973; Schopf, 1993; Brocks et al., 1999; Des Marais, 2000). The oxidized iron precipitated initially as hydrated, amorphous primary Fe(III) phases which re-crystallized during diagenesis (Klein, 2005). Anaerobic iron-reducing bacteria possibly contributed to the formation of magnetite (Lovley et al., 1987; Nealson and Myers, 1990; Konhauser et al., 2005). The accumulations of the precipitated minerals occurred in anoxic depths well below the photic zone (Klein, 2005). As cyanobacteria increased in abundance and much of the reduced iron was consumed, oxygen accumulated, ultimately producing an oxic atmosphere (Cloud, 1973). The oxygenation of the atmosphere is likely to have proceeded with much more complexity with several changes due to different forces occurring over time (Holland, 2006; Kasting, 2006).

Recent recognition of the ability of anoxygenic photosynthetic bacteria (both green and purple bacteria) to oxidize Fe(II) directly (Widdel et al., 1993; Ehrenreich and Widdel, 1994; Heising et al., 1999) supports speculation that oxidized iron in BIFs could have been produced by ancestral photoferrotrophs in the absence of molecular oxygen (Hartman, 1982; Kump, 1993; Pierson, 1994; Konhauser et al., 2002). Such organisms could have contributed oxidized iron to BIFs before the process of cyanobacterial oxygen production had evolved. The appearance of oxidized iron in an otherwise anoxic world is therefore not necessarily evidence for oxygenic photosynthesis. Evidence from some BIFs (Beukes, 2004; Tice and Lowe, 2004) and studies with purple bacteria (Kappler and Newman, 2004) support this interpretation.

Some theories about the evolution of photosynthesis include photoferrotrophy as a probable evolutionary step in the development of oxygenic photosynthetic capability in ancestral cyanobacteria (Pierson and Olson, 1989; Pierson, 1994; Olson and Blankenship, 2004; Olson, 2006). Some extant cyanobacteria may also oxidize iron directly without oxygen production (Cohen, 1984; Pierson et al., 1999; Olson, 2006). Direct anoxygenic oxidation of iron by ancestral cyanobacteria may have been pervasive in the Precambrian. Furthermore a common ancestor to both proteobacteria and cyanobacteria may have been a photoferrotroph (Olson and Blankenship, 2004). Ancestral organisms such as these, that are not known today, may have contributed substantially to BIFs.

We can only speculate about which kinds of early phototrophic microbes dominated Precambrian environments. The relative importance of each process discussed above in the formation of BIFs is unknown. It is likely that no single mechanism completely explains the deposition of all BIFs or even any particular formation. Even slight changes in environmental conditions such as light quality and intensity, pH, and redox state are particularly relevant to iron(II) oxidation by both abiotic and biotic processes. The proximity of the microbial populations and the depth of the Fe(II) source are also important. Such changes occurring locally within a basin, between different basins, and over time (even short seasonal periods of time) could favor one mechanism over another. Depending on conditions, several different mechanisms could operate simultaneously in the same environment, just as occurs in many environments on Earth today. It is very difficult to reconstruct the details of the depositional environment for most BIFs (Klein, 2005) let alone detect evidence for local spatial and temporal variations in environmental conditions that would have had an impact on a microbial scale.

### 1.2. Study site

The mats we studied in Chocolate Pots Hot Springs in Yellowstone National Park are a natural and diverse microbial ecosystem with both oxygenic and anoxygenic phototrophs. These springs provide a single high iron environment in which to quantitatively assess the contribution of both anoxygenic (direct) and oxygenic (indirect) photosynthetic processes to iron(II) oxidation under natural conditions (Pierson et al., 1999; Pierson and Parenteau, 2000). Our studies *in situ* permitted assessment of the natural biological capacity for Fe(II) oxidation in an environment in which iron tolerant photosynthetic bacteria were constantly exposed to high concentrations of Fe(II) similar to estimated Precambrian ocean values (Klein, 2005).

In Chocolate Pots Hot Springs the water at the highest temperature sources (50–54 °C) is anoxic, lacks sulfide, and is high in Fe(II) and Mn(II). The mats at the sources remain anoxic except when doing oxygenic photosynthesis. Most other anoxic environments exposed to sunlight (hot springs, stratified lakes, marine basins, and marine micro-

bial mats) are rarely high in dissolved Fe(II) and often experience large pH fluctuations and high sulfide concentrations (Revsbech and Ward, 1984; Castenholz et al., 1990; Des Marais, 1995; Wieland et al., 2005). Since sulfide reacts with oxygen and iron, it is necessary to study an environment devoid of $H_2S/HS^-$. The hot springs at Chocolate Pots are not depositional analogues for BIFs. However, the mats in these springs are suitable models for studying the biogeochemical process of Fe(II) oxidation mediated by microbial photosynthesis as it might have occurred in some marine environments including mats or ocean waters in the Precambrian.

The investigations included analysis of the microbial mat composition, *in situ* microelectrode measurements, and closed-system incubation experiments using cell suspensions prepared from homogenized mat. With the *in situ* measurements, the effects of sunlight intensity and quality on microbial Fe(II) oxidation were analyzed, and we measured the cyanobacterial oxygen production capacity in a natural environment exposed to high Fe(II). The closed-system experiments estimated the total Fe(II) oxidation rate on a cellular basis and compared cellular rates of iron(II) oxidation under different conditions. We quantified the cyanobacterial oxidation activity relative to iron(II) oxidation requirements for formation of BIFs and compared it to rates obtained for anoxygenic phototrophs and chemotrophic bacteria (Konhauser et al., 2002).

## 2. MATERIAL AND METHODS

### 2.1. *In situ* measurements

A needle-like glass solid state voltammetric gold amalgam (Au/Hg) working microelectrode (Brendel and Luther, 1995; Luther et al., 1999) along with a solid state Ag or Ag/AgCl reference and Pt counter electrode was coupled to a DLK-100A AIS Inc. electrochemical analyzer. The electrodes were made waterproof as described in Luther et al. (2001). This three electrode system allowed for simultaneous *in situ* quantitative analysis of dissolved $O_2$, $H_2O_2$, $H_2S$, thiosulfate, Fe(II), Mn(II), polysulfides and qualitative analysis of Fe(III) and soluble FeS clusters. The working electrode was constructed from 100 μm gold wire and encased in borosilicate glass with a total diameter of gold and glass near 200 μm. The glass was drawn by a glass blower and was symmetrical around the long axis. This diameter is sufficient to probe the mat as we did not see any problems with any experiments conducted in the light, in IR light or in the dark; i.e. no atmospheric $O_2$ was added across the air–water and water–mat interface to oxidize the Fe(II). The shape of the profiles and the *in situ* kinetic mat experiments clearly indicate that the electrode's tip size was not a problem.

Current versus concentration standard curves were obtained at the mat temperature with standards for each chemical species as per Brendel and Luther (1995), Luther et al. (2002) and Luther et al. (in press) and were then used to calculate the *in situ* concentrations of Fe(II), Mn(II) and oxygen. The typical operating mode was cyclic voltammetry (CV) or linear sweep voltammetry (LSV) at a scan rate of 1000 mV $s^{-1}$ over the potential range of −0.1 to −1.8 to −0.1 V. Before scanning, a conditioning step was applied at −1.0 V for 2–5 s followed by a second conditioning step at −0.1 V for 2 s. The first conditioning step removes any Mn(II), Fe(II), Fe(III) or sulfide that may be present from the Au/Hg surface. The detection limits for $O_2$, Fe(II) and Mn(II) are 3 μM at these temperatures and operating conditions. For peaks that are near in potential we used commercial software as in Brendel and Luther (1995) or the voltammetry manufacturer's advanced analysis package to discriminate and quantify peaks. Taking the derivative of the CV or LSV voltammograms also provides peak and baseline information for quantification.

The microelectrode (Fig. 1a) was mounted on a manually operated micromanipulator in 2002 (0.1 mm increments) and a remotely controlled micromanipulator in 2003 and 2004, which enabled high resolution profiling (up to 0.05 mm increments). Three to five cyclic voltammogram or linear sweep scans were recorded at each depth. During the experiments, the natural light regime was manipulated by positioning an aluminum tripod with a black cloth shroud above the study area. A window frame (27 × 30 cm) in this shroud accommodated various light filters. Besides full sunlight (no filter) and total darkness (black cloth), neutral density screens were used to provide a light intensity range between 4% and 84% of full sunlight. An infrared filter (FRF 700) (Westlake Plastics, Lenni, PA) was used to exclude all visible light while transmitting the complete solar NIR spectrum used by anoxygenic phototrophs including *Chloroflexus* sp.

To determine the effects of light intensity, an electrode was positioned within the mat at the depth of maximum oxygen production. A pyranometer light sensor with a range of 400–1100 nm (LI-200SB) connected to a Radiometer (LI-185B), LI-COR, (Linclon, NE) was positioned to measure light intensity at the surface of the mat next to the electrode. The mat was kept in the dark under the shroud and a voltammogram was taken every 6 s. The light intensity was then increased incrementally by using a combination of various neutral density filters. Thirty-two different surface light intensity levels were created and 8–12 scans were run before switching to each new light intensity.

Microprofiles of pH were measured using a combination needle pH microelectrode with a tip diameter of 0.7–0.9 mm (#818, Diamond General, Ann Arbor, MI) connected to an Oyster pH/mV meter (Extech Instruments, Waltham, MA). The electrode was calibrated at the *in situ* temperature. The temperature of the source water overlying the mat was measured using a Fluke 52K/J thermometer (Palatine, IL).

### 2.2. Closed-system incubation experiments

Small mat samples were collected and kept moist with spring water in Petri dishes for transport to the lab (Fig. 1b). The mat samples were kept in the dishes moistened with spring water and maintained at reduced levels

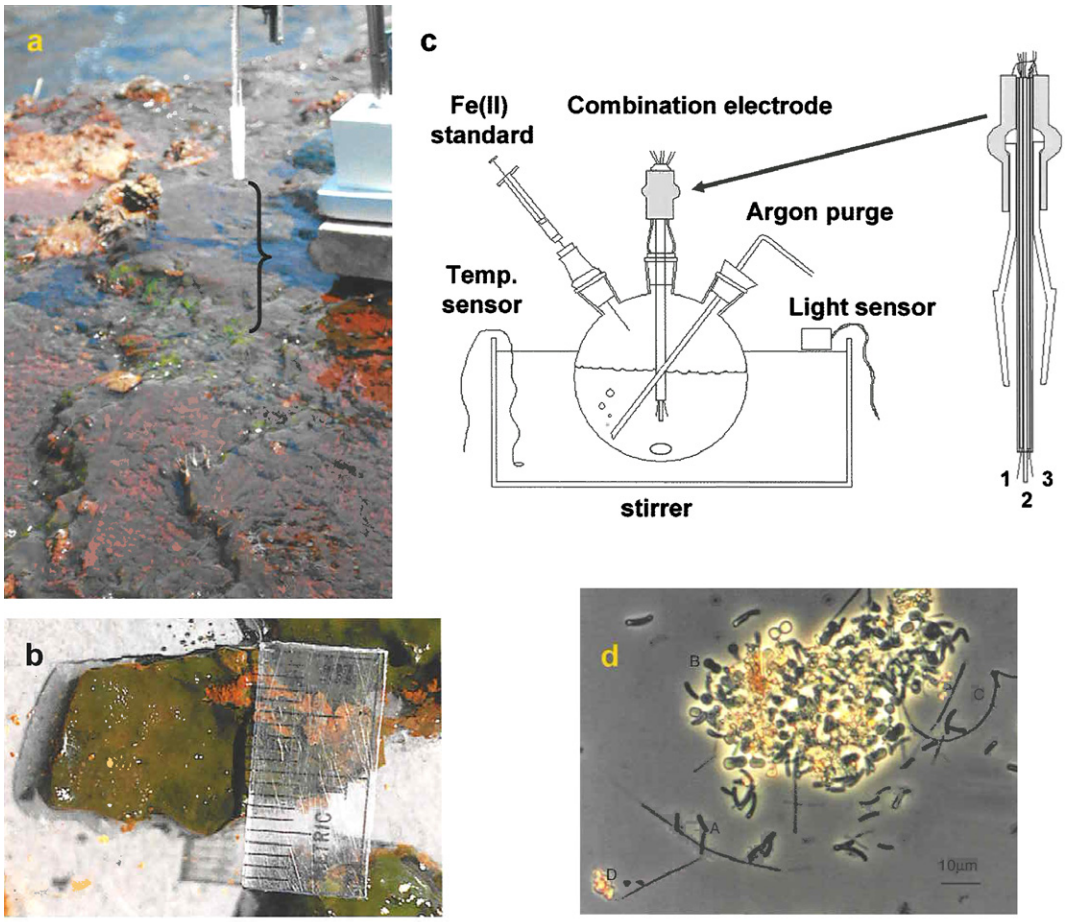


Fig. 1. Techniques and microbial characteristics of the mats used in this study. (a) Typical microelectrode as it is being placed into the mat. Bracket indicates the length of the thin part of the working electrode. (b) Photograph of a section of mat similar to those homogenized to make the cell suspensions used in (c). The orange deposit next to the ruler is ferrihydrite found beneath the mat when the green microbial layer was peeled back. (c) The incubation cell for mat suspension work is a three necked round bottom borosilicate glass flask with 19/22 ground glass joints that seal the cell's contents from $O_2$ in the atmosphere; the combination electrode with the working, reference and counter electrodes isolated in one holder. (d) Phase contrast micrograph of the microbial mat at 53 °C showing the three dominant species: *Synechococcus* sp. (A), *Cyanothece minnervae* (B), *Chloroflexus aurantiacus* (C), and the mineral ferrihydrite (D).

of light and temperature. Mat samples for the experiments reported here were stored from 1 to 10 days. No loss of photosynthetic activity was observed with up to 3 weeks of storage. Masses of cells were separated from the larger ferrihydrite sediment particles under a dissecting microscope with forceps. The cells were gently homogenized manually with a glass tissue homogenizer to avoid cell breakage and were suspended in filtered hot spring source water. Prior to use, the source water was purged with air to oxidize all Fe(II). The particulate Fe(III) was removed by pressure filtration (0.2 μm). The cell suspension was transferred to a three-neck round bottom flask in a water bath at 50–53 °C (Fig. 1c). In one experiment (data in Section 3.9 and Fig. 11) a custom-made voltammetric combination electrode (the working, reference and counter electrodes were isolated in one holder as in Fig. 1c) was mounted in the flask to simultaneously analyze the dissolved Mn(II), Fe(II) and oxygen concentration over time without the interference of atmospheric oxygen entrainment. The cell suspension was stirred with a magnetic stir bar and purged with Ar in the dark (using the same black shroud system as in the field) to remove dissolved oxygen from the suspension. A standard Fe(II) solution was injected through a septum to reach a final concentration of 200–250 μM. The black shroud was removed to admit sunlight.

In the experiments discussed in Section 3.9 (Fig. 10), the cell suspension was sparged with a gas mixture of 5% $CO_2$ and 95% $N_2$ instead of Ar to maintain a lower pH. In these experiments, the oxygen was measured with a needle oxygen electrode (768-22, Diamond General, Ann Arbor, MI) using a 2-point calibration. The Fe(II) concentration was determined by removing 0.250 ml aliquots with a syringe needle through the septum and assaying the iron with ferrozine (Pierson et al., 1999). One experiment was done with artificial light using a Hansatech LS2H tungsten halogen lamp.

The pH of the cell suspensions was measured and the cell concentrations were determined using an improved Neubauer chamber hemocytometer.

## 3. RESULTS AND DISCUSSION

### 3.1. Study location and mat composition

Chocolate Pots Hot Springs are located along the Gibbon River approximately 5 km south of Norris Geyser Basin in Yellowstone National Park. The source waters of all springs are anoxic, high in dissolved Mn(II) (50–125 μM) and Fe(II) (50–200 μM), but lack $H_2S$ (<100 nM). The springs flow over colorful siliceous iron deposits that are composed primarily of ferrihydrite and are low in manganese content (Pierson et al., 1999; Wade et al., 1999; Parenteau and Cady, 2003, 2004). Phototrophic microbial mats 0.5–2 mm thick occur about 20 cm from the spring sources (Fig. 1b). These mats are submerged beneath ~1 cm of rapidly flowing (5–10 cm/s) anoxic spring water with a temperature of 50–53 °C and a pH of 5.4–6.2.

Phase contrast microscopy (Fig. 1d), fluorescence microscopy, and spectroscopic analysis of the photosynthetic pigments in sonicated mat samples (Pierson and Parenteau, 2000) were used to identify the photosynthetic microbes in the mats shown in Fig. 1a and b. The primary phototrophic population was comprised of two cyanobacteria (*Synechococcus* sp. and *Cyanothece minervae*) and the anoxygenic phototroph *Chloroflexus* sp. Previous studies examined the composition and distribution of the bacteria within the mats (Pierson and Parenteau, 2000). The *in vivo* absorption spectrum of these mats (data not shown) was consistent with the presence of these species and similar to a previously published spectrum (Pierson and Parenteau, 2000) with maxima at 801 and 870 nm (Bchl *a*) and 737 nm (Bchl *c*) both in *Chloroflexus*. Maxima at 679 nm (Chl *a*) and 620 nm (phycocyanin) were due to cyanobacteria. Carotenoids present in the phototrophs contributed to a broad maximum from 400 to 500 nm.

### 3.2. Light and dark *in situ* profiles

In voltammetry, the applied potential (Volts) identifies the species via the half-wave potential ($E_{1/2}$) at which the electrode reaction occurs (confirmed with standards added to the source waters), while the signal current (Ampere) is a measure of the species concentration. The voltammetric scans obtained *in situ* at various depths showed that the source water just above the mat (Fig. 2, −0.2 mm depth) was characterized by soluble Fe(II) ($E_{1/2} = -1.30$ V) and Mn(II) ($E_{1/2} = -1.45$ V) and that oxygen ($E_{1/2} = -0.3$ V) and hydrogen sulfide ($E_{1/2} = -0.6$ V) were not present. A voltammogram obtained at the surface of the mat (Fig. 2, depth 0.0 mm) showed a trace of oxygen indicated by the S-shaped curve at $E_{1/2} = -0.3$ V and the presence of electroactive Fe(III) ($E_{1/2} = \sim -0.5$ V), presumably Fe(III) complexed with organic ligands as the peak current on consecutive scans showed no significant change as it does for inorganic Fe(III) (Taillefert et al., 2000).

In the mat (Fig. 2, depth 0.1 mm), the oxygen signal became more evident and a Fe(II) signal could not be detected; notice the horizontal baseline at −1.3 V (arrow). During the detection of oxygen, oxygen is reduced to peroxide at the electrode surface and the formed peroxide is reduced to water at a potential of $E_{1/2} = -1.1$ V, indicated by the S-shaped peroxide signal equivalent in size to the oxygen signal detected at −0.3 V.

The oxygen concentration reached a maximum at a depth of 0.5 mm in the mat and decreased as shown by the scans at 0.6 mm, 1.3 mm and 2.0 mm depth (Fig. 2). The manganese signal was present and did not decrease throughout the profile. The rate of abiotic manganese oxidation at a pH of ~6 is low (Stumm and Morgan, 1996).

A pair of profiles measured in 2002 (Fig. 3a and b) show the main characteristics of dissolved Fe(II), Mn(II), and $O_2$ distributions with depth in the light and dark. In the dark (Fig. 3a), $O_2$ was absent. The concentration of Fe(II) ranged from 50 to 75 μM and there was little variation in dissolved Fe(II) concentration from the mat surface to its base. The concentration of Mn(II) ranged from about 40 μM at the surface of the mat to more than 100 μM near the base. Most values remained between 50 and 100 μM and were highest below a depth of 1.0 mm. In the light (Fig. 3b), the $O_2$ concentration increased dramatically just beneath the mat surface (0.1 mm) and reached its maximum value (190 μM) at a depth of 0.5 mm. The $O_2$ concentration decreased sharply at a depth of 1.0 mm and fell to near zero at the base of the mat. The change from dark to light did not substantially affect the Mn(II) concentration profile (Fig. 3a and b). Conversely, the Fe(II) concentration profile in the light (Fig. 3b) changed dramatically from the one measured in the dark (Fig. 3a). In the light, Fe(II) was still present in surface waters above the mat (~80 μM), but decreased to below detection (<3 μM) at depths where $O_2$ exceeded 25 μM. The pH profiles showed a narrow range (pH $6 \pm 0.2$) at all depths independent of light conditions (Fig. 3a and b).

In other profiles measured in 2002 (Fig. 3c and d) and 2004 (Fig. 3e and f), the Fe(II) decrease was also directly coupled to the appearance of free dissolved oxygen. Dissolved Fe(II) and oxygen did not co-occur at any depth within the mat. The magnitude of variance in the replicate readings at each depth in Fig. 3e and f was less than in Fig. 3a and b. In Fig. 3f, the Mn(II) concentration remained constant throughout the profile and was the same as the surface water concentration of approximately 50 μM. Slight variations observed among the profiles were likely due to changes in the thickness and hydrology within the mat. Fe(II) concentrations in the source waters varied from hot spring to hot spring and year to year. The overall patterns of distribution, however, were similar among the different hot springs and over several years (2002–2004).

Atmospheric $O_2$ was not a significant factor in this system. These mats were near the hot spring source and the dark measurements showed that no $O_2$ was in the water above the mats in the absence of photosynthesis (Fig. 3a, c, and e). Thus, atmospheric $O_2$ could not be responsible for the observed Fe(II) oxidation when the mat was switched from darkness to light. Under light conditions, some of the $O_2$ produced within the mat diffused upward into the overlying flowing water resulting in low measurable $O_2$ concentrations in some cases (Fig. 3b). The Fe(II) concentration in the overlying water remained high in both dark and light experiments (Fig. 3) but was completely oxi-

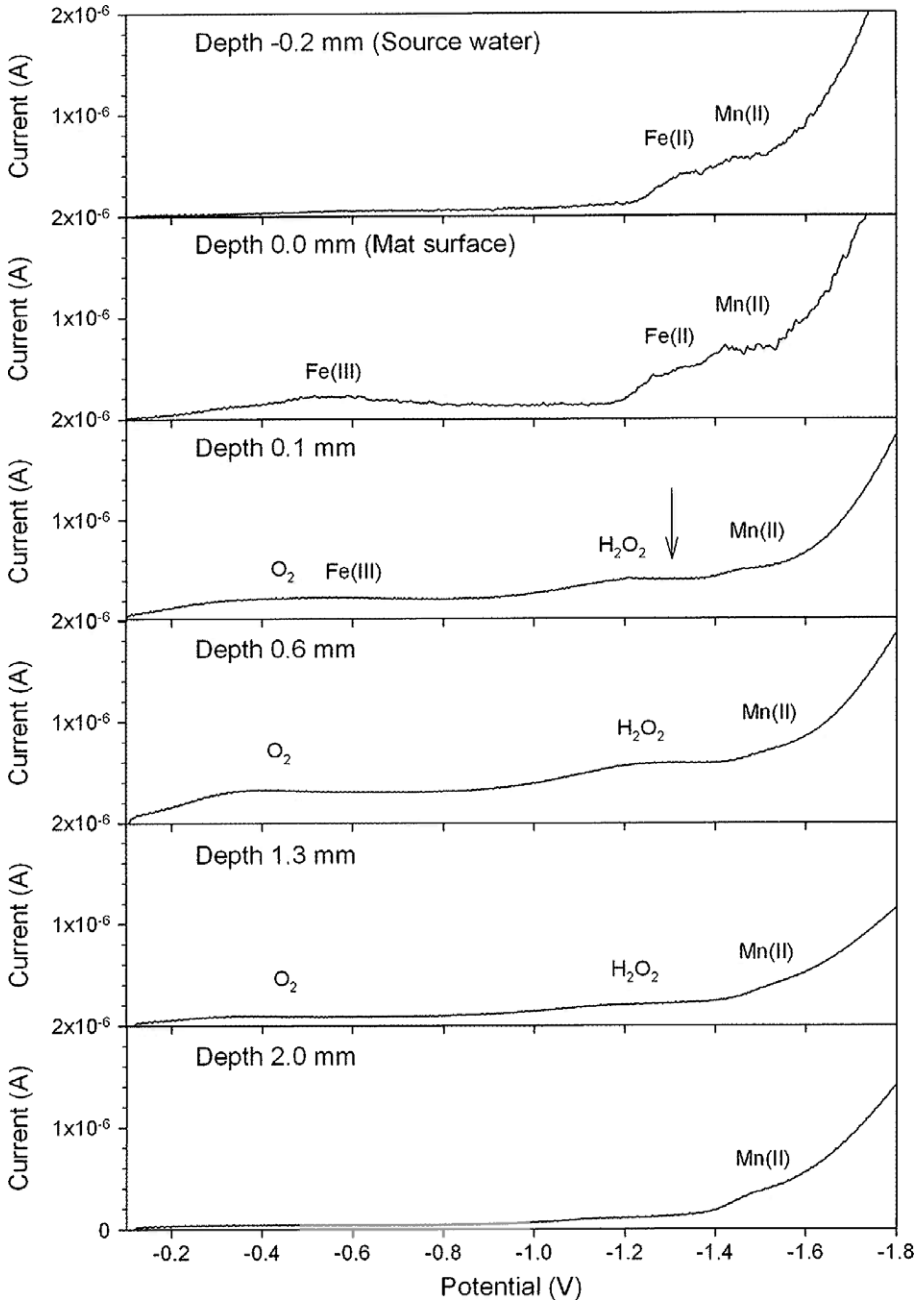


Fig. 2. Selection of characteristic *in situ* voltammograms at various depths in the mat (July, 2002). The reference was an uncoated Ag wire in saturated KCl solution.

dized in the light in the top mm of the mat where the phototrophs reside. Since the source water lacked $O_2$ and $H_2S$, but was high in Fe(II), we observed the impact of oxygenic photosynthesis on Fe(II) oxidation, distinct from the influence of sulfide and atmospheric $O_2$. We are not aware of any other field studies in which this has been possible.

### 3.3. The role of pH

Changes in pH can affect the rate of Fe(II) and Mn(II) oxidation (Stumm and Morgan, 1996). In many cyanobacterial mat studies, pH is higher in the light than in the dark due to $CO_2$ consumption by photosynthesis (Pierson et al., 1999). In our experiments, however, the pH was nearly constant in light and dark (Fig. 3a and b). Two conditions could contribute to this observation: (A) The thin mats were continually flushed by the low pH source water and (B) the high rate of oxygen-dependent Fe(II) oxidation, which follows a 4Fe(II):1$O_2$ stoichiometry (Eq. (1)), produces both an Fe(III)

$$10H_2O + 4Fe^{2+} + O_2 \rightarrow 4Fe(OH)_3 + 8H^+ \quad (1)$$

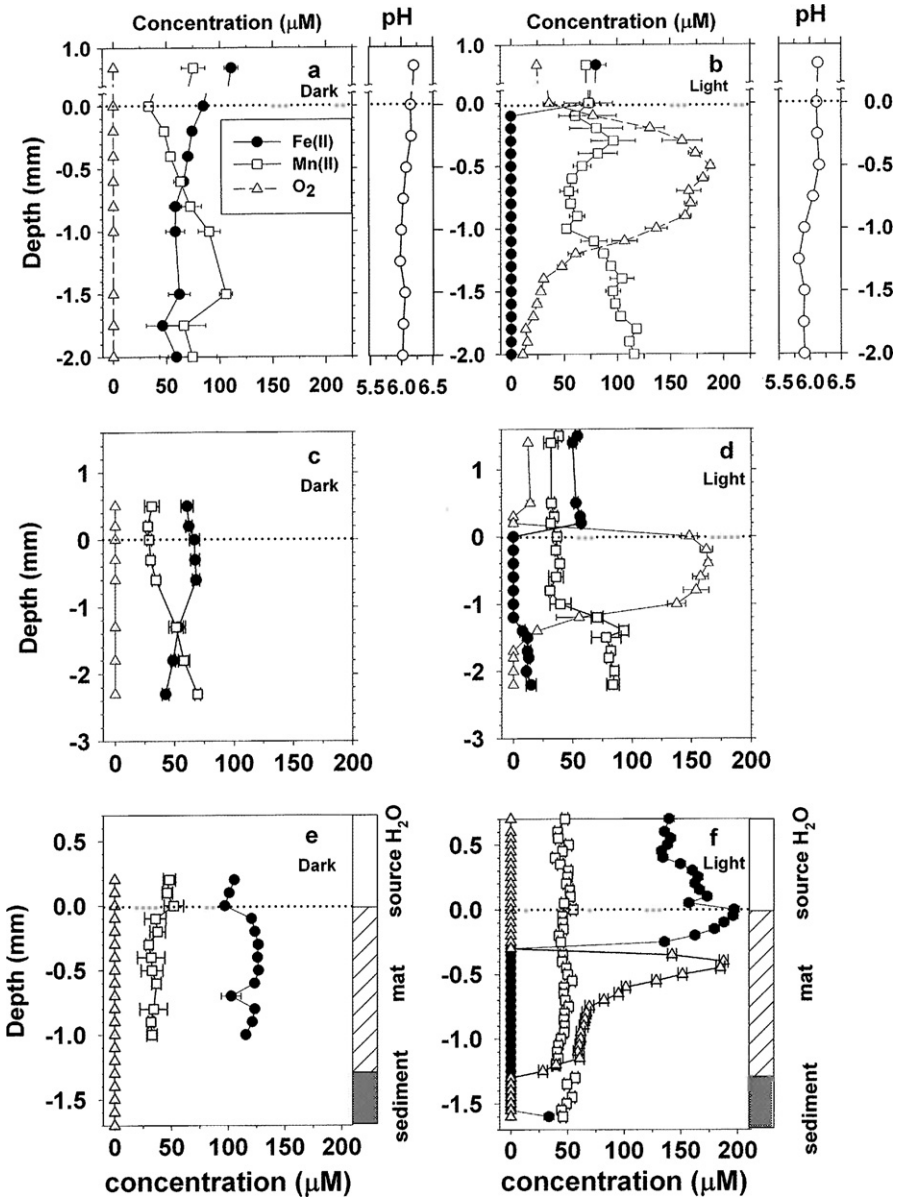


Fig. 3. Voltammetric microelectrode dark (a,c,e) and light (b,d,f) profiles in three different hot spring mats measured at 50–53 °C. (a,b) Profiles at South Mound Tree site June 2002. Each point is mean value of 4 measurements with SD. pH profiles also included. (c,d) Profiles at Main Mound site in June, 2002. Each point is mean value of 4 measurements with SD. (e,f) Profiles at Main Mound site in July 2004. In E each point is mean of 3 measurements with SD. In F each measurement value is the average of 5–9 measurements with SD.

solid phase and protons (Stumm and Morgan, 1996) keeping the pH relatively low and near constant. Consequently pH changes did not contribute to the increased rate of Fe(II) oxidation in the light.

### 3.4. The stability of Mn

Abiotic Mn(II) oxidation by $O_2$ is very slow at the prevailing environmental conditions (pH ~6, temperature ~50 °C), whereas Fe(II) oxidation is fast (Stumm and Morgan, 1996; Luther, 2005). The complete oxidation of Fe(II) and lack of oxidation of Mn(II) in Chocolate Pots hot springs (Fig. 3) is consistent with the high iron concentrations and low manganese concentrations observed in most BIFs (0–2.5 wt%) (Anbar and Holland, 1992; Kump and Holland, 1992; Horstmann and Halbich, 1995; Rao and Naqvi, 1995). The minerals deposited at Chocolate Pots are also low in manganese (Parenteau and Cady, 2003, 2004). In Precambrian marine environments, once all Fe(II) had been oxidized, continued oxygenic photosynthesis by cyanobacteria could have raised the pH substantially thereby increasing the rate of Mn(II) oxidation and manganese deposition. Such activity would have resulted in a spatial and/or temporal separation of iron and manganese deposits (Holland, 1984; Kump and Holland, 1992). Although it is theoretically possible for a phototroph to oxidize Mn(II) di-

rectly in photosynthesis (Pierson, 1994), we saw no evidence for this process or for bacterial chemotrophic oxidation of Mn(II).

### 3.5. *In situ* analysis of Fe(II) oxidation rates

*In situ* microelectrode experiments were designed to quantify the rate of Fe(II) oxidation by photosynthetically produced $O_2$ within the mats. The microelectrode was embedded in the mat at the depth of maximum oxygen concentration and production (~0.5 mm). The light was switched from dark (3.5 W/m$^2$) to full sunlight (620 W/m$^2$) and back to dark. Fig. 4 follows the response of the Fe(II) concentrations to these changes in light. The data points in Fig. 4 were calculated from voltammograms similar to those shown in Fig. 5. Fe(II) did not disappear immediately after a shift from dark to light, but experienced a short lag period perhaps as the cyanobacteria acclimated to light. After this lag period the Fe(II) concentration dropped from 66 μM to below detection (<3 μM) within 60 s (Fig. 4). The rate of Fe(II) oxidation was 1.60 μM Fe(II)/s. The re-appearance of Fe(II) after the switch from light to dark was associated with a 16 s lag period due to the titration of remaining excess $O_2$ by Fe(II) entering the mat from the flowing water. After 90 s in the dark, the initial Fe(II) concentration of 66 μM was re-established.

The oxidation of Fe(II) at 0.5 mm within the mat was rapid and complete. At this depth the mat had 9 times the amount of $O_2$ needed for total Fe(II) removal. All of the Fe(II) in the source water (~66 μM; Fig. 4) could be oxidized and precipitated with only ~17 μM $O_2$. This $O_2$/Fe(II) ratio (9:1) measured in the mat exceeds the 1:4 stoichiometric ratio in Eq. (1) and suggests that, at 0.5 mm, a pseudo-first order Fe(II) oxidation process may occur (Stumm and Morgan, 1996). Some excess $O_2$ from the mat diffused into the overlying water (Fig. 3b).

Analysis of the decay in Fe(II) concentration with time as light was allowed to reach the mat (Fig. 4) indicates that the data fit a zeroth order rate law for all eight decay points with a slope, $k_0$, of −1.60 μM/s ($t_{1/2} = \{[Fe(II)]_i/(2k)\} = 20.3$ s; $r^2 = 0.983$). A first order decay is only observed for the last five decay points where $r^2 = 0.967$, $k_1 = -0.108$ s$^{-1}$ and $t_{1/2} = 6.40$ s. A zeroth order reaction is consistent with light being the primary limiting factor as the concentration of $O_2$ is dependent on light intensity and photosynthesis.

The voltammetric scans for another experiment that followed the changes in oxygen concentration accompanying the changes in Fe(II) concentration (Fig. 5) show that in the dark, the mat environment reflected the source water chemical composition, dissolved iron(II) and Mn(II) were high and no dissolved oxygen was present (Fig. 5, $T = 0$). Sunlight was admitted at $T = 0$ (Fig. 5). Soon after full sunlight was admitted (Fig. 5, $T = 11$ s), the Fe(II) concentration dropped rapidly, and after 29 s, dissolved $O_2$, Fe(III) organic complexes and peroxide signals appeared, but a Fe(II) signal was not detected. The oxygen, Fe(III) organic complexes and peroxide signal increased over time (Fig. 5; $T = 11$ s, $T = 29$ s and $T = 58$ s) to a more constant level at $T = 111$ s.

When these changes in both Fe(II) and $O_2$ concentration are followed with time (Fig. 6), it can be seen that the oxygen rises in the light (Fig. 6a) only after the Fe(II) approaches zero. The oxygen fell rapidly after the shift to darkness (Fig. 6b). Fe(II) then rose only after $O_2$ reached zero (Fig. 6b). The re-appearance of Fe(II) after the switch from light to dark was associated with a 40 s lag period in this case. The Fe(II) oxidation rate in Fig. 6a again fit a zeroth order reaction (with a slope, $k_0$, of −6.40 μM/s; $t_{1/2} = \{[Fe(II)]_i/(2k)\} = 7.42$ s; $r^2 = 1.000$) and the zeroth order rate constant was four times higher in this experiment (6.40 μM Fe(II)/s) than the previous one in Fig. 4.

Further evidence for excess oxygen production was found in the depth profiles. The upper $O_2$ depth gradient (Fig. 3b) is ~430 μM $O_2$/mm over 0.5 mm vs a Fe(II) removal at the surface of the mat of ~700 μM Fe(II)/mm over 0.1 mm. This gradient ratio of about two Fe(II) to one $O_2$ indicates excess $O_2$, which can sustain an abiotic reaction with Fe(II), according to Eq. (1) with some loss of excess $O_2$ to the overlying water.

Even in this dynamic natural environment, the measured Fe(II) oxidation rates (1.60 and 6.40 μM Fe(II)/s) (Fig. 4 and 6) are in close agreement with laboratory experiments for abiotic Fe(II) oxidation (rates ranging from 1.7 to

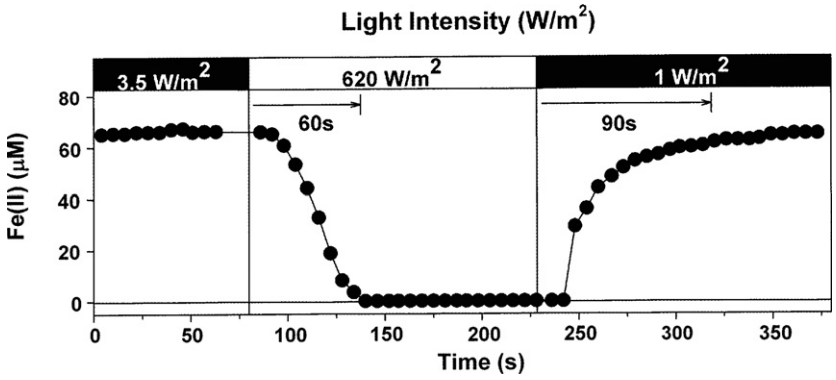


Fig. 4. Response time for changes in Fe(II) concentration as a function of changing light conditions (shown in upper bar). Fe(II) concentration was measured over time with the voltammetric microelectrode positioned in the mat at the depth of maximum $O_2$ production (0.5 mm) to determine a maximum Fe(II) removal rate and the response time (2003).

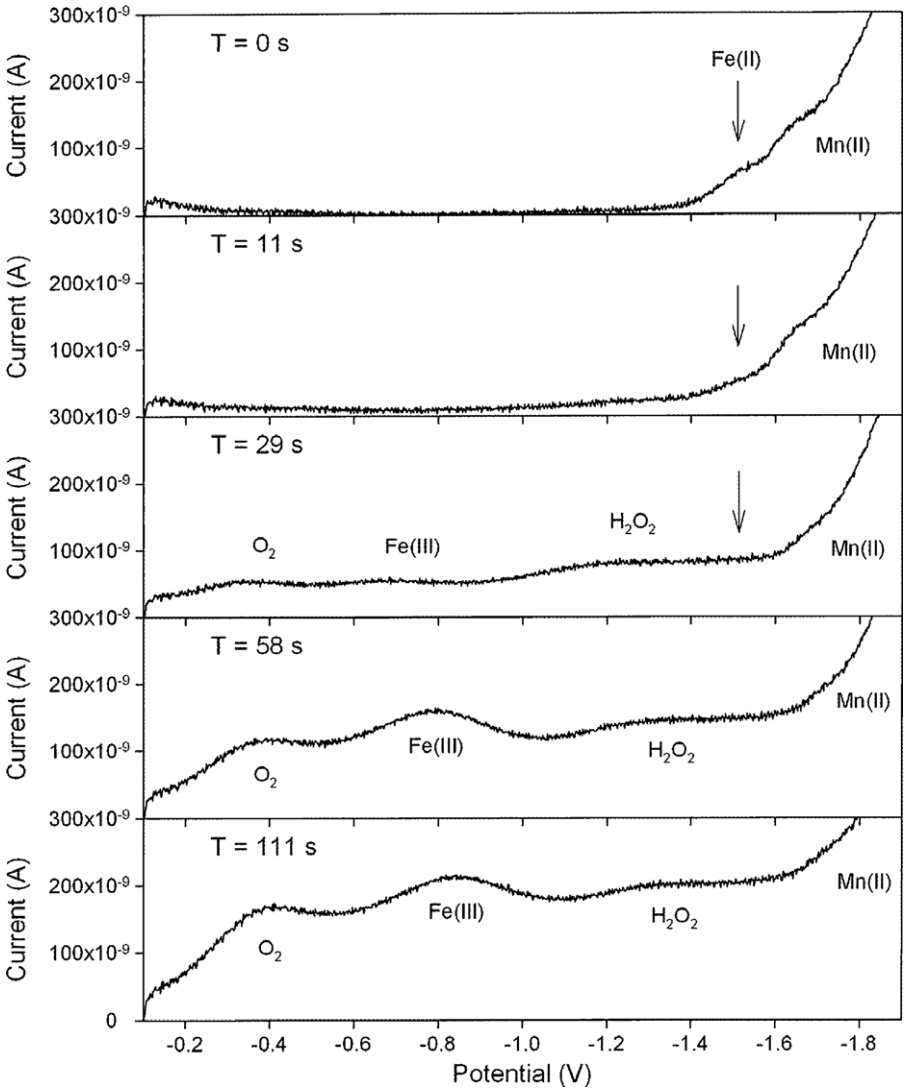


Fig. 5. Selected *in situ* voltammograms showing the progression of $O_2$, $H_2O_2$, Fe(III), Fe(II), and Mn(II) concentrations over time after a shift (at $T = 0$ s is when light was introduced) from dark conditions ($\sim$3 W/m$^2$) to full light conditions (1000 W/m$^2$). The reference was an Ag wire coated with AgCl in saturated KCl solution (Ag/AgCl).

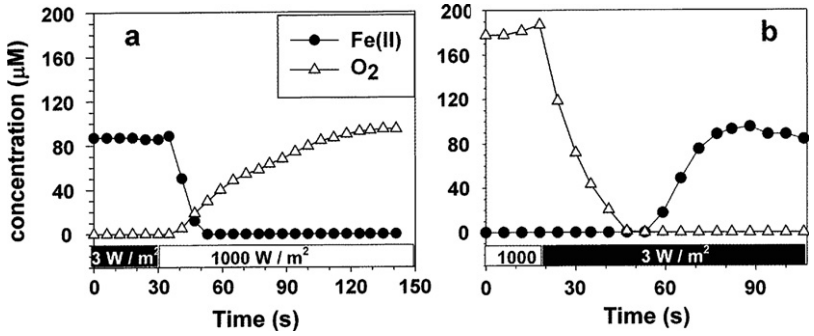


Fig. 6. Changes in Fe(II) and oxygen concentration as a function of changing light conditions (shown in bottom bar) measured over time with the voltammetric microelectrode positioned in the mat at the depth of maximum $O_2$ production ($\sim$0.5 mm). The scans in Fig. 5 contributed data points to panel a. (a) Steady state values measured in dark and then shifted to full sunlight. (b) Steady state values measured in full sunlight and then shifted to dark.

9.4 μM Fe(II)/s when extrapolated to 50 °C) (Sung and Morgan, 1980). The similarity of these rates to our measured rates supports an abiotic mechanism for Fe(II) oxidation consistent with the absence of chemotrophic iron oxidizers in these mats (Emerson and Weiss, 2004). These observations support our conclusion, that rapid Fe(II) oxidation is primarily a chemical process mediated by cyanobacterial oxygen production in Chocolate Pots Hot Springs.

### 3.6. Assessment of Fe(III) in mats

Fe(III) signals due to soluble organic–Fe(III) complexes (Taillefert et al., 2000) formed during oxidation of Fe(II) were detected during the light regimes (Figs. 2 and 5). Although this signal was observed in many profiles in the zone of maximum oxygen production, it could not be quantified as every organic–Fe(III) compound has a different current vs concentration slope. Its presence is, however, evidence that Fe(II) oxidation occurred with formation of soluble organic–Fe(III) species prior to Fe(III) precipitation.

### 3.7. Light intensity effects

We measured the dependence of *in situ* Fe(II) concentrations at 0.5 mm depth into the mat on light intensity change at the surface of the mat. After switching to each new light intensity, the mat stabilized quickly as determined by voltammetry [8–12 scans were recorded until the last 5 were reproducible]. The last measured scans at each intensity were then used to calculate Fe(II) and $O_2$ concentrations (Fig. 7). Even at very low surface light levels of ~55 W/m$^2$, dissolved Fe(II) was oxidized in the center of the mat (~0.5 mm depth) (Fig. 7). At a light level of ~85 W/m$^2$ (only 7.1% of the maximum surface intensity of 1200 W/m$^2$), sufficient oxygen was produced to remove all dissolved Fe(II) (see insert Fig. 7). This suggests that dissolved Fe(II) entering into the mat can be actively oxidized soon after sunrise and that even on overcast days (~150 W/m$^2$) there can be sufficient light for total Fe(II) oxidation. The response of Fe(II) oxidation to light intensity further confirms the role of cyanobacterial photosynthesis.

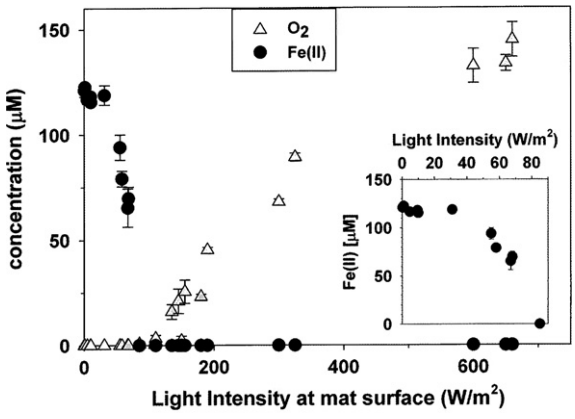


Fig. 7. Dissolved Fe(II) and oxygen concentrations measured at 0.5 mm depth into the mat and at different light intensities. (Inset) dissolved Fe(II) scaled to lower light intensities.

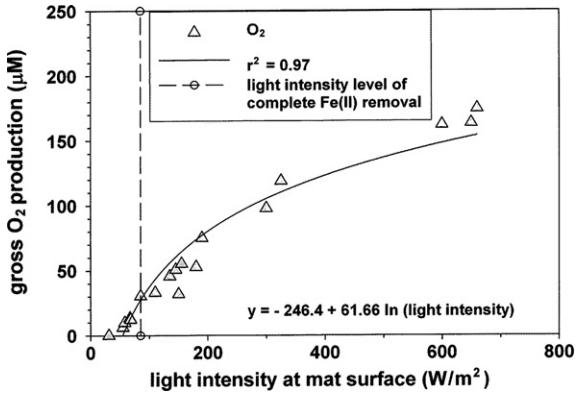


Fig. 8. Gross oxygen production versus light intensity, modeled according to a natural log curve. The vertical line indicates that complete Fe(II) removal occurs at $\geqslant$85 W/m$^2$.

The gross oxygen production (defined as the $O_2$ concentration that would be detected at a given light intensity if Fe(II) oxidation did not occur) at 0.5 mm vs light intensity was approximated with a natural log model (Fig. 8) showing first oxygen production occurred at a surface intensity of 55 W/m$^2$ which is only 4.6% of the maximum surface light available. The cyanobacteria and iron minerals strongly attenuate visible radiation within the mat. At a depth of 0.5 mm, the available radiation is much less than the 55 W/m$^2$ measured at the surface (Pierson and Parenteau, 2000). Hence cyanobacteria are capable of substantial oxygen production resulting in complete Fe(II) oxidation at very low light intensities.

### 3.8. Near infrared (NIR) radiation and Fe(II) oxidation

An *in situ* depth profile of Fe(II) was measured in the dark and with an infrared filter (blocking all radiation below 700 nm). The dark and NIR profiles were nearly identical (Fig. 9) indicating that NIR radiation did not support the anoxygenic photosynthetic oxidation of Fe(II) in these mats. We have previously shown that NIR penetrates better than visible radiation in cyanobacterial mats and iron sediments (Pierson et al., 1999; Pierson and Parenteau, 2000). Radiation at wavelengths less than 700 nm is strongly attenuated by the cyanobacteria and ferrihydrite. NIR can be used only by bacteriochlorophyll-containing anoxygenic photosynthetic bacteria and not by cyanobacteria. Restricting the light environment to NIR radiation thus prevents oxygen production. Anoxygenic phototrophs such as some purple and green bacteria (Widdel et al., 1993; Heising et al., 1999) can oxidize Fe(II) directly without producing oxygen. Although the anoxygenic *Chloroflexus* present in these mats is not known to oxidize Fe(II), it seemed possible that it might in this high iron environment (Pierson et al., 1999). Since no evidence was found for the oxidation of Fe(II) in the presence of NIR radiation, if *Chloroflexus* is capable of such activity, there is insufficient biomass present to contribute measurably to the total iron(II) oxidation in

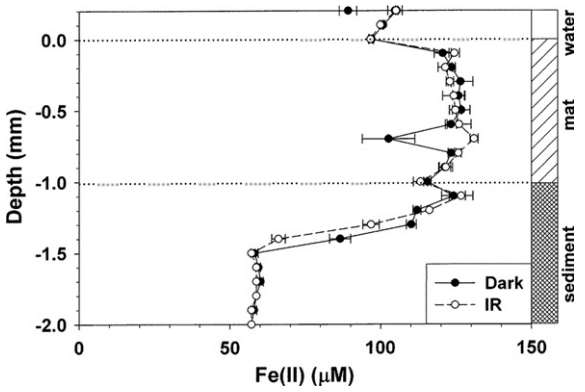


Fig. 9. Depth profiles of Fe(II) concentration measured during dark conditions and in the presence of an infrared filter.

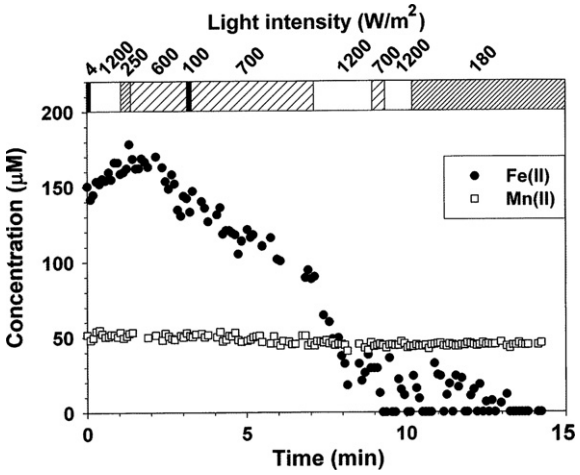


Fig. 11. Closed system incubation experiment. Cyanobacterial cell suspension at pH 7.0 and sunlight intensities indicated on the top *x*-axis. Dissolved Fe(II) and Mn(II) measured with voltammetric microelectrode.

these mats. It appears that *Chloroflexus* may be growing in Chocolate Pots primarily as a photoheterotroph dependent on organic substrates produced by cyanobacteria, just as it does in most other hot spring environments where it forms more conspicuous mat layers (Revsbech and Ward, 1984).

### 3.9. Closed system incubation experiments with mat suspensions

The closed system incubations were done with homogenized cell suspensions in flasks to simulate a planktonic distribution of cells, to calculate the rate of Fe(II) oxidation under controlled conditions, and to determine the rate of Fe(II) oxidation per cell. In two experiments (Fig. 10a and b), oxygen levels were measured with an oxygen specific electrode and Fe(II) was measured with the ferrozine assay. In another experiment (Fig. 11), oxygen, Fe(II), and Mn(II) were measured with voltammetry.

The dark/light shift experiment with an abiotic control (Fig. 10a) showed that photosynthesis is required for the light-dependent oxidation of Fe(II). Oxygen accumulates only after nearly all the iron is oxidized. The abiotic control using the same spring water with added Fe(II) but without the cells showed little decrease in Fe(II) and no increase in oxygen (Fig. 10a). The slight decrease in Fe(II) was due to the inadvertent introduction of oxygen during sample removal for the ferrozine assay. In the presence of cyanobacteria the Fe(II) decreased and accompanying oxygen increased, when switched from dark to light, showing the same relationship as when measured *in situ* with the electrode embedded at a depth of 0.5 mm in the mat (Fig. 6a). In the cell suspension simulating a planktonic distribution, however, the level of oxygen attained after oxidation of all the Fe(II) was much less than in the dense microbial mat. The experiment in Fig. 10a was done in artificial light (350 W/m$^2$). A second experiment (Fig. 10b) done in natural sunlight (700 W/m$^2$) also showed that the presence of the cyanobacteria was required for rapid Fe(II) oxidation. Rates from this experiment are in Table 1. In both of these experiments, sparging with $N_2/CO_2$ kept the pH low (5.3–5.5).

Experiments with the voltammetric electrode permitted acquisition of many more data points during the period

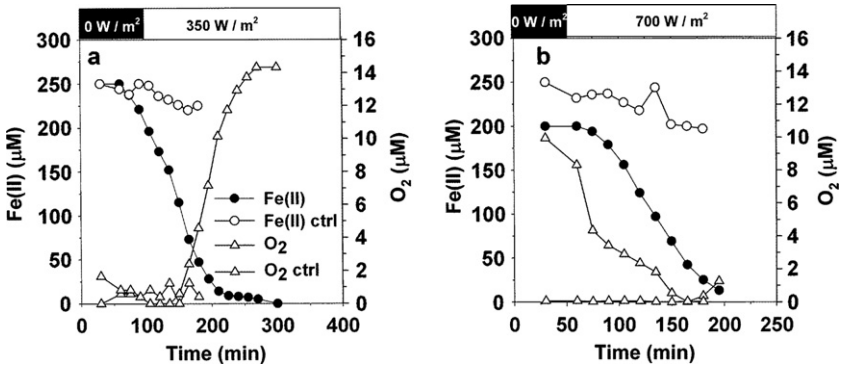


Fig. 10. Closed system incubation experiments with homogenized mat suspensions. Cyanobacterial cell suspensions compared with abiotic controls. $O_2$ measured with an electrode and Fe(II) with ferrozine assay. (a) Cyanobacterial cell suspension and abiotic control both at pH 5.5 and 350 W/m$^2$ from tungsten–halogen lamp. (b) Cyanobacterial cell suspension and abiotic control both at pH 5.3 and 700 W/m$^2$ natural sunlight.

Table 1
Fe(II) oxidation rates from mat suspensions relative to BIF deposition

| Fig. | Light level ($W/m^2$) | pH | Cell density ($10^6$ cells/ml) | Fe(II) oxidation rate ($10^{-16}$ mol Fe/cell/min) | Fe(II) oxidation rate ($10^{-12}$ mol Fe/cell/yr) | Cyanobacterial cells to deposit $4.5 \times 10^{12}$ mol Fe/yr ($10^{+20}$ cells) | Productive surface area necessary (%) |
|---|---|---|---|---|---|---|---|
| 11 | 1200 | 7 | 5.35 | 101 | 2654 | 17.1 | 2 |
| 11 | 700 | 7 | 5.35 | 27 | 710 | 63.2 | 6 |
| 10b | 700 | 5.3 | 5.93 | 2.9 | 76 | 596 | 60 |

of rapid iron(II) oxidation for better rate determinations (Fig. 11). Since samples did not have to be taken for iron analysis, problems with inadvertent introduction of oxygen during sampling were avoided. These simulated planktonic suspensions were sparged with Ar and the pH was 7.0. Within approximately 8–9 min of being exposed to sunlight, all of the added 200 μM Fe(II) was removed from solution (Fig. 11). The concentration of dissolved Mn(II) remained constant (~50 μM) over the course of the experiment confirming the observations made with the *in situ* profiles (Fig. 3).

The fluctuations in light intensity during the experiment in Fig. 11 were caused by intermittent cloud cover. The variations in light regime directly affected the Fe(II) removal rate. Therefore, only data measured during the more stable light conditions (first 700 $W/m^2$ period, and the second period of 1200 $W/m^2$) were used to estimate Fe(II) oxidation rates. The rate per cell at 700 $W/m^2$ was 27% of the rate per cell at 1200 $W/m^2$ (Table 1). The rapid impact of light intensity on oxidation rate, clearly shows the dependence of Fe(II) oxidation on photosynthesis. Rates of Fe(II) oxidation decreased not only at lower light intensities, but also at lower pH. At the same light intensity (700 $W/m^2$), the rate per cell at pH 5.3 was about 10% of that at pH 7.0 (Table 1).

### 3.10. Quantitative assessment of Iron(II) oxidation in mat suspensions relative to BIFs

The BIFs of the Hamersley Basin of Western Australia are a large sequence formed about 2.5 Ga that have a depositional structure consistent with chemically precipitated iron (Klein, 2005). One possible source of oxidizing power is molecular oxygen from cyanobacterial photosynthesis (Trendall, 1983; Olson, 2006).

Using the measured cellular Fe(II) oxidation rates per min from the planktonic simulation experiments shown in Fig. 1c and described in Section 3.9 (Table 1) and assuming an average 12 h light and 12 h dark period per day, we calculated an annual oxidation rate of $7.1 \pm 3 \times 10^{-10}$ mol Fe(II) oxidized/cell at 700 $W/m^2$ and $26.5 \pm 2 \times 10^{-10}$ mol Fe(II) oxidized/cell at 1200 $W/m^2$ (Table 1).

Konhauser et al. (2002) calculated a depositional rate of $4.53 \times 10^{12}$ mol Fe/year for the $1 \times 10^{11}$ $m^2$ area of the Hamersley basin. Dividing this estimated annual Fe(III) deposition rate by the annual cellular Fe(II) oxidation rates, we obtained the number of cyanobacterial cells needed to oxidize the iron to form one annual layer (varve). At pH 7.0 this value ranged from $1.7 \pm 0.16 \times 10^{21}$ cells at a light intensity of 1200 $W/m^2$ to $6.3 \pm 0.3 \times 10^{21}$ cyanobacterial cells at 700 $W/m^2$ (Table 1). At pH 5.3 and 700 $W/m^2$, approximately $6 \times 10^{22}$ cells are needed (Table 1). These numbers are 1–2 orders of magnitude lower than the numbers of cells required of anoxygenic phototrophic or aerobic chemotrophic bacteria (Konhauser et al., 2002). Assuming an average depth of 100 m for the photic zone over the entire area of the Hamersley Basin, a cyanobacterial cell density of $1.7 \pm 0.02 \times 10^2$ cells/ml at 1200 $W/m^2$ or $6.3 \pm 0.3 \times 10^2$ cells/ml at 700 $W/m^2$ would be sufficient to oxidize all the required Fe(II) (Table 1). At pH 5.3 and 700 $W/m^2$ the required cell concentration would be $5.96 \times 10^3$ cells/ml (Table 1). With a shallower photic zone of only 10 m, these densities remain in the range of $10^3$ to $10^4$ cells/ml. If we assume a higher cell density of $10^4$ cells/ml (Konhauser et al., 2002) comparable to contemporary seawater concentrations of cyanobacteria (See et al., 2005) and a photic zone depth of 100 m, the photosynthetically productive surface area required to oxidize all of the depositional iron would be 2% of the entire basin at 1200 $W/m^2$ and 6% at 700 $W/m^2$ (Table 1). Even at pH 5.3 and 700 $W/m^2$ only 60% of the basin area would need to be productive (Table 1). At lower light intensities, a higher percentage of the area would be required.

While there are many variables to be considered in Fe(II) oxidation and BIF deposition, and we have ignored the additional complexities of iron cycling (Konhauser et al., 2005), these working estimates are useful in confirming the potential of oxygenic photosynthesis to oxidize a large amount of iron. We do not need to invoke vast dense cyanobacterial mats nor high density planktonic blooms to oxidize the Fe(II). A modest proportion of the basin or a shallower photic zone with relatively low cell densities across the entire basin can produce the required deposition of iron.

The data from lower pH values are included in these calculations to illustrate the environmental range over which some cyanobacteria are capable of efficiently producing oxygen and oxidizing iron. While it may not be known precisely at what pH Precambrian Fe(II) oxidation occurred, our data show that Fe(II) could have been oxidized by cyanobacterial photosynthesis at least over the pH range of 5.3–7.0.

## 4. CONCLUSIONS AND IMPLICATIONS

The data from both *in situ* mat studies and closed system incubation experiments led to the same conclusion for the high temperature mats at Chocolate Pots hot springs. Light was the primary variable determining Fe(II) oxidation by controlling the $O_2$ production through cyanobacterial photosynthesis. The photosynthetically induced Fe(II) removal was rapid and complete.

These data have some implications for the potential role of oxygenic photosynthesis in Fe(II) oxidation during the Precambrian. We recognize that the microbial mats at Chocolate Pots are not analogous to the Precambrian ocean environments in which deposition of BIFs occurred. However, these mats are the best microbial environment we have found in which to quantitatively assess the potential role of cyanobacteria in indirect abiotic Fe(II) oxidation. The biogeochemical analyses reported here can be cautiously applied to the Precambrian environment when considering some of the conditions below. We believe they provide experimental justification for keeping cyanobacterial oxygenic photosynthesis in the mix of possible mechanisms to account for deposition of at least some BIFs.

We have recognized that several mechanisms may have been involved in the oxidation of Fe(II) in the Precambrian. Konhauser et al. (2002) have presented the case for the quantitative role of anoxygenic phototrophs and chemotrophic bacteria. In some basins under some conditions, anoxygenic phototrophs may have had a greater role than oxygenic cyanobacteria (Kappler et al., 2005). In some other environments, cyanobacteria may have had a greater role. In others, coexistence of all three biological mechanisms in stratified or mixed communities may have resulted in complex contributions and even interactions in Fe(II) oxidation. Light penetration in oceanic waters affects the distribution of phototrophs and is influenced by many factors including the presence of microorganisms and the chemical composition of the water. For example, the strong UV absorption by soluble Fe(II) and suspended nanoparticulate Fe(III) assemblages could protect microorganisms from damaging UV radiation in shallower depths (Olson and Pierson, 1986; Pierson et al., 1993; Pierson, 1994). Cyanobacteria are versatile organisms and are well adapted to harvesting wide ranges of the visible spectrum. Early cyanobacteria could have used wavelengths of light in the red regions with chlorophyll *a* and phycocyanin. They were also well adapted to growing deeper in the water column using the Soret band of chlorophyll, possibly carotenoids, and the light-harvesting phyocerythrins. The versatility of cyanobacteria includes the abilities to grow beneath anoxygenic phototrophs and to grow anoxygenically themselves (Gorlenko et al., 1987; Pierson, 1994). Anoxygenic photosynthesis using iron(II) or manganese(II) is certainly a likely capability of ancestral cyanobacteria and may have had a role in some Precambrian BIF deposition.

Our studies presented here provide an opportunity for the quantitative assessment of the potential role of oxygenic cyanobacterial photosynthesis in the oxidation of Fe(II) and the subsequent precipitation of Fe(III) during the Precambrian.

## ACKNOWLEDGMENTS

We thank G. K. Druschel, Jes Werner, L. Shanks, T. S. Moore and A. Packer for technical assistance in the field. We thank Doug Nixon for making the borosilicate glass portion of the solid state voltammetric microelectrodes. This work was supported by a NASA Exobiology grant, a sub-contract to the University of Puget Sound from the NASA Astrobiology grant to Arizona State University, and a subcontract to the University of Delaware from the NASA Astrobiology grant to University of California, Berkeley. We acknowledge partial support from the National Oceanic and Atmospheric Administration Office of Sea Grant (NA05OAR4171041). We wish to thank K. Konhauser and two anonymous reviewers for their comments which improved the paper. We thank Yellowstone National Park for permission to do research at Chocolate Pots Hot Springs.

## REFERENCES

Anbar A. D. and Holland H. D. (1992) The photochemistry of manganese and the origin of banded iron formations. *Geochim. Cosmochim. Acta* **56**, 2595–2603.

Berkner L. V. and Marshall L. C. (1964) The history of growth of oxygen in the Earth's atmosphere. In *The Origin and Evolution of Atmospheres* (eds. P. J. Brancazio and A. G. W. Cameron). Wiley, New York.

Beukes N. (2004) Early options in photosynthesis. *Nature* **431**, 522–523.

Braterman P. S., Cairns-Smith A. G. and Sloper R. W. (1983) Photo-oxidation of hydrated $Fe^{2+}$–significance for banded iron formations. *Nature* **303**, 163–164.

Brendel P. J. and Luther, III, G. W. (1995) Development of a gold amalgam voltammetric microelectrode for the determination of dissolved Fe, Mn, $O_2$, and S(−II) in porewaters of marine and fresh-water sediments. *Environ. Sci. Technol.* **29**, 751–761.

Brinkman R. T. (1969) Dissociation of water vapor evolution of oxygen in terrestrial atmosphere. *J. Geophy. Res.* **74**, 5355–5368.

Brocks J. J., Logan G. A., Buick R. and Summons R. E. (1999) Archean molecular fossils and the early rise of eukaryotes. *Science* **285**, 1033–1036.

Cairns-Smith A. G. (1978) Precambrian solution photochemistry, inverse segregation, and banded iron formations. *Nature* **76**, 807–808.

Castenholz R. W., Bauld J. and Jørgensen B. B. (1990) Anoxygenic microbial mats of hot springs: thermophilic *Chlorobium* sp.. *FEMS Microbiol. Ecol.* **74**, 325–336.

Cloud P. (1965) Significance of the Gunflint (Precambrian) microflora. *Science* **148**, 27–35.

Cloud P. E. (1973) Paleoecological significance of banded iron-formations. *Econ. Geol.* **68**, 1135–1143.

Cohen Y. (1984) Comparative N and S cycles. In *Current Perspectives in Microbial Ecology* (eds. M. J. Klug and C.A. Reddy). Amer. Soc. for Microbiol., Washington, DC.

Des Marais D. J. (1995) The biogeochemisty of hypersaline microbial mats. *Adv. Microb. Ecol.* **14**, 251–274.

Des Marais D. J. (2000) Evolution—when did photosynthesis emerge on Earth? *Science* **289**, 1703–1705.

Ehrenreich A. and Widdel F. (1994) Anaerobic oxidation of ferrous iron by purple bacteria, a new type of phototrophic metabolism. *Appl. Environ. Microbiol.* **60**, 4517–4526.

Emerson D. and Revsbech N. P. (1994a) Investigation of an iron-oxidizing microbial mat community located near Aarhus, Denmark: field studies. *Appl. Environ. Microbiol.* **60**, 4022–4031.

Emerson D. and Revsbech N. P. (1994b) Investigation of an iron-oxidizing microbial mat community located near Aarhus, Denmark: laboratory studies. *Appl. Environ. Microbiol.* **60**, 4032–4038.

Emerson D. and Weiss J. (2004) Bacterial iron oxidation in circumneutral freshwater habitats: findings from the field and the laboratory. *Geomicrobiol. J.* **21**, 405–414.

François L. M. (1986) Extensive deposition of banded iron formations was possible without photosynthesis. *Nature* **320**, 352–354.

Gorlenko V. M., Starynin D. A., Bonch-Osmolovskaya E. A. and Kachalkin V. I. (1987) Production processes in microbial cenoses of the Thermofil'NYI Hot Springs. *Mikrobiologiya* **56**, 872–878.

Hartman H. (1982) The evolution of photosynthesis and microbial mats: a speculation on the banded iron formations. In *Microbial Mats, Stromatolites* (eds. Y. Cohen, R. W. Castenholz and H. O. Halvorson). Alan R. Liss, New York.

Heising S., Richter L., Ludwig W. and Schink B. (1999) *Chlorobium ferrooxidans* sp. nov., a phototrophic green sulfur bacterium that oxidizes ferrous iron in coculture with a "*Geospirillum*" sp. strain. *Arch. Microbiol.* **172**, 116–124.

Holland H. D. (2006) The oxygenation of the atmosphere and the oceans. *Phil. Trans. R. Soc. B* **361**, 903–915.

Holland H. D. (1984) *The Chemical Evolution of the Atmosphere and Oceans*. Princeton University Press, Princeton.

Holm N. G. (1987) Biogenic influences on the geochemistry of certain ferruginous sediments of hydrothermal origin. *Chem. Geol.* **63**, 45–57.

Horstmann U. E. and Halbich I. W. (1995) Chemical-composition of banded iron-formations of the Griqualand West sequence, Northern Cape-Province, South-Africa, in comparison with other Precambrian iron formations. *Precambrian Res.* **72**, 109–145.

Kappler A. and Newman D. K. (2004) Formation of Fe(III)-minerals by Fe(II)-oxidizing photoautotrophic bacteria. *Geochim. Cosmochim. Acta* **68**, 1217–1226.

Kappler A., Pasquero C., Konhauser K. O. and Newman D. K. (2005) Deposition of banded iron formations by anoxygenic phototrophic Fe(II)-oxidizing bacteria. *Geology* **68**, 1217–1226.

Kasting J. F. (2006) Ups and downs of ancient oxygen. *Nature* **443**, 643–645.

Klein C. (2005) Some Precambrian banded iron-formations (BIFs) from around the world: their age, geologic setting, mineralogy, metamorphism, geochemistry, and origin. *Am. Mineral.* **90**, 1473–1499.

Klein C. and Beukes N. J. (1992) Time distribution, stratigraphy, and sedimentologic setting, and geochemistry of Precambrian Iron-Formations. In *The Proterozoic Biosphere: A Multidisciplinary Study* (eds. J. W. Schopf and C. Klein). Cambridge University Press, Cambridge.

Konhauser K. O., Newman D. K. and Kappler A. (2005) The potential significance of microbial Fe(III) reduction during deposition of Precambrian banded iron formations. *Geobiology* **3**, 167–177.

Konhauser K. O., Hamade T., Raiswell R., Morris R. C., Ferris F. G., Southam G. and Canfield D. E. (2002) Could bacteria have formed the Precambrian banded iron formations? *Geology* **30**, 1079–1082.

Kump L. (1993) Bacteria forge a new link. *Nature* **362**, 790–791.

Kump L. R. and Holland H. D. (1992) Iron in Precambrian rocks—implications for the global oxygen budget of the ancient Earth. *Geochim. Cosmochim. Acta* **56**, 3217–3223.

Lovley D. R., Stolz J. F., Nord, Jr., G. L. and Phillips E. J. P. (1987) Anaerobic production of magnetite by a dissimilatory iron-reducing microorganism. *Nature* **330**, 252–254.

Luther, III, G. W. (2005) Manganese(II) oxidation and Mn(IV) reduction in the environment—two one-electron transfer steps versus a single two-electron step. *Geomicrobiol. J.* **22**, 195–203.

Luther, III, G. W., Reimers C. E., Nuzzio D. B. and Lovalvo D. (1999) In situ deployment of voltammetric, potentiometric and amperometric microelectrodes from a ROV to determine $O_2$, Mn, Fe, S(−2) and pH in porewaters. *Environ. Sci. Technol.* **33**, 4352–4356.

Luther G. W., Rozan T. F., Taillefert M., Nuzzio D. B., Di Meo C., Shank T. M., Lutz R. A. and Cary S. C. (2001) Chemical speciation drives hydrothermal vent ecology. *Nature* **410**, 813–816.

Luther, III, G. W., Bono A., Taillefert M. and Cary S. C. (2002) A continuous flow electrochemical cell for analysis of chemical species and ions at high pressure: laboratory, shipboard and hydrothermal vent results. In *Environmental Electrochemistry: Analyses of Trace Element Biogeochemistry*, vol. 811 (eds. M. Taillefert and T. Rozan). American Chemical Society Symposium Series. American Chemical Society, Washington, DC, pp. 54–73 (Chapter 4).

Luther, III, G. W., Glazer B. T., Ma S., Trouwborst R. E., Moore T. S., Metzger E., Kraiya C., Waite T. J., Druschel G., Sundby B., Taillefert M., Nuzzio D. B., Shank T. M., Lewis B. L. and Brendel P. J. (in press) Use of voltammetric solid-state (micro)electrodes for studying biogeochemical processes: laboratory measurements to real time measurements with an *in situ* electrochemical analyzer (ISEA). *Marine Chemistry*, doi:10.1016/j.marchem.2007.03.002.

Nealson K. H. and Myers C. R. (1990) Iron reduction by bacteria: a potential role in the genesis of banded iron formations. *Am. J. Sci.*, 35–45.

Olson J. M. (2006) Photosynthesis in the Archean Era. *Photosynth. Res.* **88**, 109–117.

Olson J. M. and Blankenship R. E. (2004) Thinking about the evolution of photosynthesis. *Photosynth. Res.* **80**, 373–386.

Olson J. M. and Pierson B. K. (1986) Photosynhesis 3.5 thousand million years ago. *Photosynth. Res.* **9**, 251–259.

Parenteau M. N. and Cady S. L. (2003) Microbial biosignatures and primary mineral phases in high iron thermal springs. *Geological Society of America*, 2003 Annual Meeting. Abstracts with Programs. **35** (6), 150.

Parenteau M. N. and Cady S. L. (2004). Natural 2-line and 6-line ferrihydrite characterization and microbial biomineralization in a high iron thermal spring. *Geological Society of America*, 2004 Annual Meeting. Abstracts with Programs **36** (5), 475.

Pierson B. K. (1994) The emergence, diversification, and role of photosynthetic eubacteria. In *Early Life on Earth* (ed. S. Bengtson) Nobel Symposium No. 84, Columbia University Press, New York.

Pierson B. K., Mitchell H. K. and Ruff-Roberts A. L. (1993) *Chloroflexus aurantiacus* and ultraviolet radiation: implications for Archean shallow-water stromatolites. *Orig. Life Evol. Biosph.* **23**, 243–260.

Pierson B. K., Olson J. M. (1989) Evolution of photosynthesis in anoxygenic photosynthetic prokaryotes. In *Microbial Mats: Physiological Ecology of Benthic Microbial Communities* (eds. Y. Cohen and E. Rosenberg). Amer. Soc. Microbiol, Washington, DC.

Pierson B. K. and Parenteau M. N. (2000) Phototrophs in high iron microbial mats: microstructure of mats in iron-depositing hot springs. *FEMS Microbiol. Ecol.* **32**, 181–196.

Pierson B. K., Parenteau M. N. and Griffin B. M. (1999) Phototrophs in high-iron-concentration microbial mats: physiological ecology of phototrophs in an iron-depositing hot spring. *Appl. Environ. Microbiol.* **65**, 5474–5483.

Rao T. G. and Naqvi S. M. (1995) Geochemistry, depositional environment and tectonic setting of the BIFs of the Late Archean Chitradurga Schist Belt, India. *Chem. Geol.* **121**, 217–243.

Revsbech N. P. and Ward D. M. (1984) Microelectrode studies of interstitial water chemistry and photosynthetic activity in a hot spring microbial mat. *Appl. Environ. Microbiol.* **48**, 270–275.

Schopf J. W. (1993) Microfossils of the Early Archean Apex Chert—new evidence of the antiquity of life. *Science* **260**, 640–646.

See J., Richardson T., Shen R., Guinasso N., Pickney J. and Campbell L. (2005) Combining new technologies for determination of phytoplankton community structure in the northern Gulf of Mexico. *J. Phycol.* **41**, 305–310.

Stumm W. and Morgan J. J. (1996) *Aquatic Chemistry; Chemical Equilibria and Rates in Natural Waters*. Wiley, New York.

Sung W. and Morgan J. J. (1980) Kinetics and product of ferrous iron oxygenation in aqueous systems. *Environ. Sci. Technol.* **14**, 561–568.

Taillefert M. A., Bono B. and Luther, III, G. W. (2000) Reactivity of freshly formed Fe(III) in synthetic solutions and marine (pore)waters: voltammetric evidence of an aging process. *Environ. Sci. Technol.* **34**, 2169–2177.

Tice M. M. and Lowe D. R. (2004) Photosynthetic microbial mats in the 3,416-Myr-Old Ocean. *Nature* **431**, 549–552.

Towe K. M. (1978) Early Precambrian oxygen—case against photosynthesis. *Nature* **274**, 657–661.

Trendall A. F. (1983) The Hamersley Basin. In *Iron Formation: Facts and Problems* (eds. A. F. Trendall and R. C. Morris). Elsevier Science Publishers, Amsterdam.

Wade M. L., Agresti D. G., Wdowiak T. J., Armendarez L. P. and Farmer J. D. (1999) A Mossbauer investigation or iron-rich terrestrial hydrothermal vent systems: lessons for Mars exploration. *J. Geophys. Res.* **104**, 8489–8507.

Widdel F., Schnell S., Heising S., Ehrenreich A., Assmus B. and Schink B. (1993) Ferrous iron oxidation by anoxygenic phototrophic bacteria. *Nature* **362**, 834–836.

Wieland A., Zopfi J., Benthien M. and Kühl M. (2005) Biogeochemistry of an iron-rich hypersaline microbial mat (Camargue, France). *Microb. Ecol.* **49**, 34–49.

*Associate editor:* Jack J. Middelburg